The FEBS Journal

FEBS PRESS science publishing by scientists

Molecular insights into the role of the polyalanine region in mediating PHOX2B aggregation

Luciano Pirone[1], Laura Caldinelli[2], Simona Di Lascio[3], Rocco Di Girolamo[4], Sonia Di Gaetano[1], Diego Fornasari[3], Loredano Pollegioni[2], Roberta Benfante[3,5] and Emilia Pedone[1]

1 Institute of Biostructure and Bioimaging, CNR, Napoli, Italy
2 Dipartimento di Biotecnologie e Scienze della Vita, Università degli studi dell'Insubria, Varese, Italy
3 Department of Medical Biotechnology and Translational Medicine, Università degli Studi di Milano, Italy
4 Department of Chemical Sciences, University of Naples Federico II, Italy
5 CNR- Neuroscience Institute, Milan, Italy

Keywords
CCHS; fibrils; PHOX2B; polyalanine expansion

Correspondence
R. Benfante, Neuroscience Institute, CNR, via Vanvitelli, 32 - 20129, Milan, Italy
Tel: +39 02 50316945
E-mail: roberta.benfante@in.cnr.it
and
E. Pedone, Institute of Biostructure and Bioimaging, CNR, Napoli, Italy
E-mail: empedone@unina.it

Luciano Pirone, Laura Caldinelli and Simona Di Lascio contributed equally to this article

(Received 21 December 2018, revised 27 February 2019, accepted 4 April 2019)

doi:10.1111/febs.14841

About 90% of congenital central hypoventilation syndrome (CCHS) patients show polyalanine triplet expansions in the coding region of transcription factor PHOX2B, which renders this protein an intriguing target to understand the insurgence of this syndrome and for the design of a novel therapeutical approach. Consistently with the role of PHOX2B as a transcriptional regulator, it is reasonable that a general transcriptional dysregulation caused by the polyalanine expansion might represent an important mechanism underlying CCHS pathogenesis. Therefore, this study focused on the biochemical characterization of different PHOX2B variants, such as a variant containing the correct C-terminal (20 alanines) stretch, one of the most frequent polyalanine expansions (+7 alanines), and a variant lacking the complete alanine stretch (0 alanines). Comparison of the different variants by a multidisciplinary approach based on different methodologies (including circular dichroism, spectrofluorimetry, light scattering, and Atomic Force Microscopy studies) highlighted the propensity to aggregate for the PHOX2B variant containing the polyalanine expansion (+7-alanines), especially in the presence of DNA, while the 0-alanines variant resembled the protein with the correct polyalanine length. Moreover, and unexpectedly, the formation of fibrils was revealed only for the pathological variant, suggesting a plausible role of such fibrils in the insurgence of CCHS.

Introduction

Almost 500 human proteins contain polyalanine (polyAla) stretches [1]. Alanine tracts are coded by imperfect trinucleotide repeats (GCN), and GCN trinucleotide expansion mutations that lead to polyAla expansions above a certain threshold cause at least nine different diseases including developmental defects and neurological disorders [2–4]. Eight out of nine known polyAla-associated diseases are caused by mutations in genes encoding for developmental transcription factors and are congenital syndromes. The ninth, oculopharyngeal muscular dystrophy, is a late-onset progressive disease caused by polyAla

Abbreviations
BS3, bis(sulfosuccinimidyl) suberate; CCHS, Congenital Central Hypoventilation Syndrome; CHX, cycloheximide; DTT, dithiothreitol; GdnHCl, guanidine hydrochloride; HD, homeodomain; IPTG, isopropyl-β-D-thiogalactoside; NLS, N-lauroylsarcosine; PABPN1, poly(A)-binding protein nuclear 1; PMSF, phenylmethylsulphonylfluoride.

expansions in the poly(A)-binding protein nuclear 1 (PABPN1) involved in mRNA polyadenylation. The exact molecular functions of the polyAla tracts remain largely unknown, and they are supposed to act as flexible spacer elements between functional protein domains, thus playing a role in protein conformation and protein–protein interactions. Given their role, several lines of evidence support that the expansions of polyAla tracts can lead to protein misfolding, cellular mislocalization, aggregation, and aberrant protein–protein interactions [5].

PHOX2B is a transcription factor that plays an essential role in the development of the autonomic nervous system and the neural structures involved in breathing control [6–8]. PHOX2B consists of 314 amino acids and it is composed by a 97-residue N-terminal domain, a central domain with a conserved 60-residue homeodomain (DNA-binding motif) and two polyAla stretches of 9 and 20 residues, respectively, within the C-terminal domain (Fig. 1). Heterozygous in-frame triplet duplications within the sequence stretch coding for the 20-alanine amino acids and the consequent polyAla expansions account for more than 90% of patients that suffer congenital central hypoventilation syndrome (CCHS, MIM# 209880). CCHS is a rare life-threatening autosomal dominant disease that is characterized by impaired autonomic respiratory control leading to hypoventilation due to abnormal ventilatory responses to hypoxia and hypercapnia [9].

The polyAla expansions described so far in CCHS patients range from a minimum of 4 additional residues to a maximum of 13 alanines, extending the wild-type 20 alanine tract to 33 alanines, and the most frequent mutations are those leading to the addition of 5, 6, and 7 alanines [10].

Several molecular mechanisms by which the polyAla expansions can cause CCHS have been proposed and include loss-of-function mechanisms, dominant-negative effects, and/or toxic gain of function of the mutant proteins [11–16]. In particular, polyAla expansions decrease PHOX2B DNA binding and transcriptional activity (in a gene-specific manner) [11,12], alter homodimer formation *in vitro* [15], and modify interactions with other proteins such as transcriptional coactivators or corepressors [16]. Alanine expansions can induce the formation of oligomers *in vitro* and in cell overexpression assays [12,14,17], that suggest protein misfolding, although cytoplasmic aggregation and PHOX2B wild-type trapping are only seen in the case of longer alanine expansions (more than +9 alanines) [11,18]. Of note, PHOX2B protein aggregates colocalize with ubiquitin and molecular chaperones (such as HSP70) [14,18]. The cytoplasmic aggregation observed in overexpression studies increased over time and decreased when the longest polyAla expanded protein (+13 alanines) was transfected using a lower amount of DNA [11,17]. The intranuclear aggregation of the +13 alanines variant was also time dependent, but inversely correlated with the amount of transfected DNA [11]. These observations, together with the apparent absence of visible aggregation of variant proteins with short expansions, suggest slower kinetics in aggregation for these variants.

In vivo, immunohistochemical analysis of the Phox2b-expressing regions of the mouse model of CCHS, obtained using a knock-in approach to introduce a +7 alanine expansion (27A), did not show any existence of aggregates, and their contribution to the disease pathogenesis is still controversial [19]. The discrepancy between the aggregation seen in overexpression analyses and the little direct evidence of this phenomenon *in vivo* is a common feature with the other disease-associated polyAla proteins, with the exception of PABPN1 that forms amyloid fibrils *in vitro* and nuclear inclusion *in vivo*, and HOXD13 that accumulates in the cytoplasm both *in vitro* and *in vivo* [20].

The mechanism of polyAla aggregation has been extensively studied *in vitro* and some studies have suggested that the polyAla sequence can form amyloid fibrils [21], whereas others showed that the resulting aggregates are α-helical structures [22,23]. Previous studies [15] on the role of polyAla expansions on the aggregation behavior of PHOX2B need to be further deepened in order to learn more about the molecular steps leading to the disease.

To this aim, we carried out biochemical comparisons of PHOX2B variants containing the correct C-terminal (20 alanines) stretch, one of the most frequent polyAla expansion (+7 alanines) or a PHOX2B variant lacking the complete C-terminal Ala stretch (0 alanines).

Results

Cloning, expression, and purification of PHOX2B (20A) and its variants

PHOX2B contains a homeodomain (HD, residues 98–157) and a peculiar C-terminal region (residues 158–314) characterized by the presence of two stretches of alanines: one made of nine (residues 159–167) and the second of 20-alanine residues (residues 241–260; polyAla motif) (Fig. 1A). Prediction of the secondary structure on the full-length protein (PHOX2B FL) by

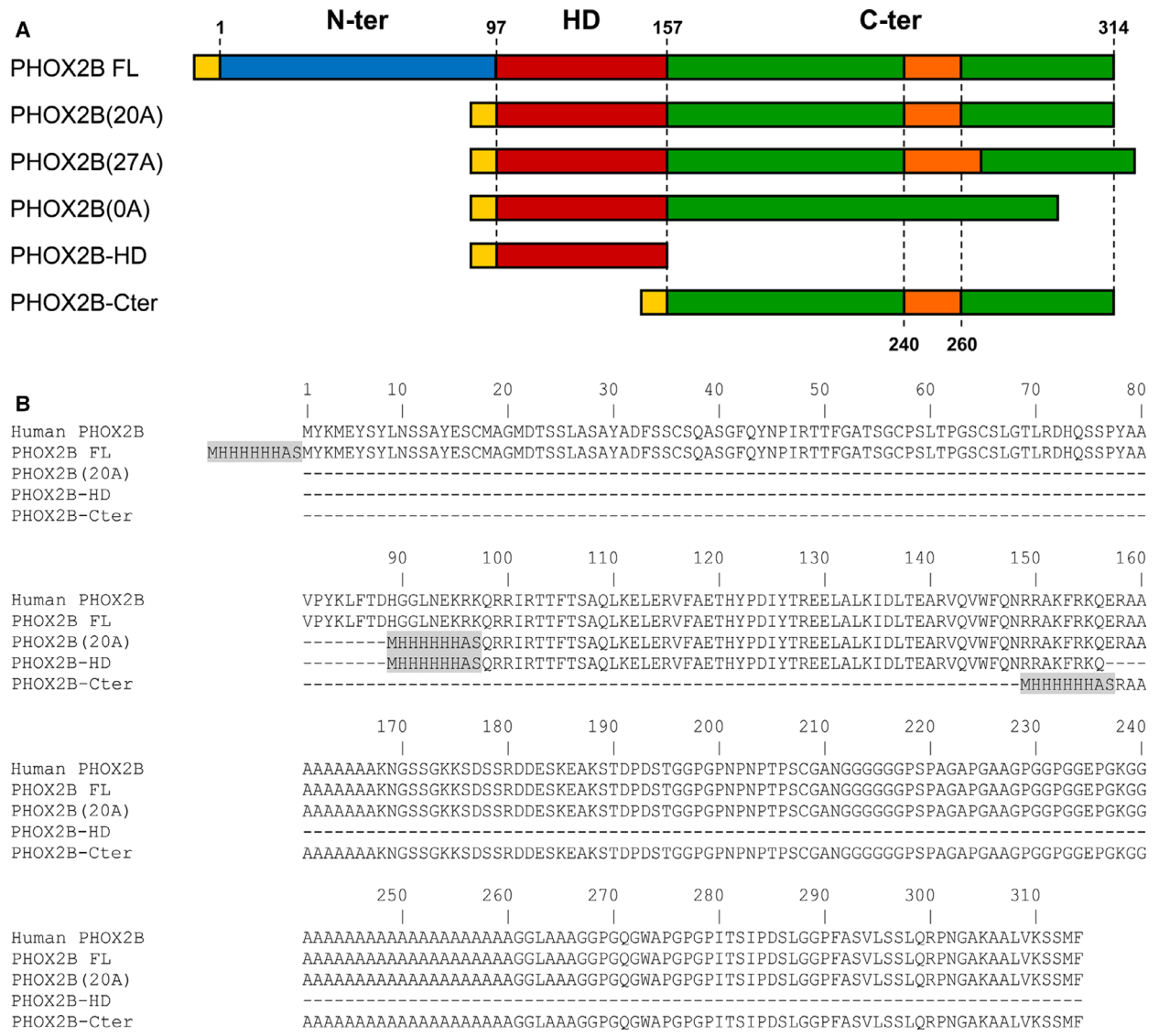

Fig. 1. (A) Schematic representation of the PHOX2B variants produced in this work. (B) Sequence comparison of produced PHOX2B variants; residues are numbered as in PHOX2B wild-type. Gray boxes: additional amino acids (MHHHHHHAS) present at the N-terminal end in the recombinant proteins.

different software unveils that the only structured region corresponds to the conserved homeodomain (residues 98–135, Fig. 2). This folded core domain is arranged in three helical regions, which canonically constitute the homeodomain, flanked by long, largely unstructured tails at both the N- and C termini.

The PHOX2B FL was achieved under denaturing conditions only: refolding by 0.1% (w/v) N-lauroylsarcosine (NLS) yielded a preparation unable to bind DNA. For this reason the experiments were performed on a deleted PHOX2B form (PHOX2B(20A), residues 98–314), lacking the N-terminal hypothetical unstructured 97 residues which could confer instability to the recombinant protein (Fig. 1A). Indeed, we focused on the characterization of fragments corresponding to the two putative domains (HD and C-terminal domain, corresponding to the sequences 98–157 and 158–314, respectively) and of two variants, namely PHOX2B (27A) corresponding to the addition of seven Ala at position 260, and PHOX2B(0A) lacking the second polyAla stretch (residues 241–260) (Fig. 1A,B). The insertion variant (named 27A) is strictly linked to the development of the congenital central hypoventilation syndrome (CCHS) [24] and the deletion variant (named 0A) was designed to clarify the role of the polyAla sequence.

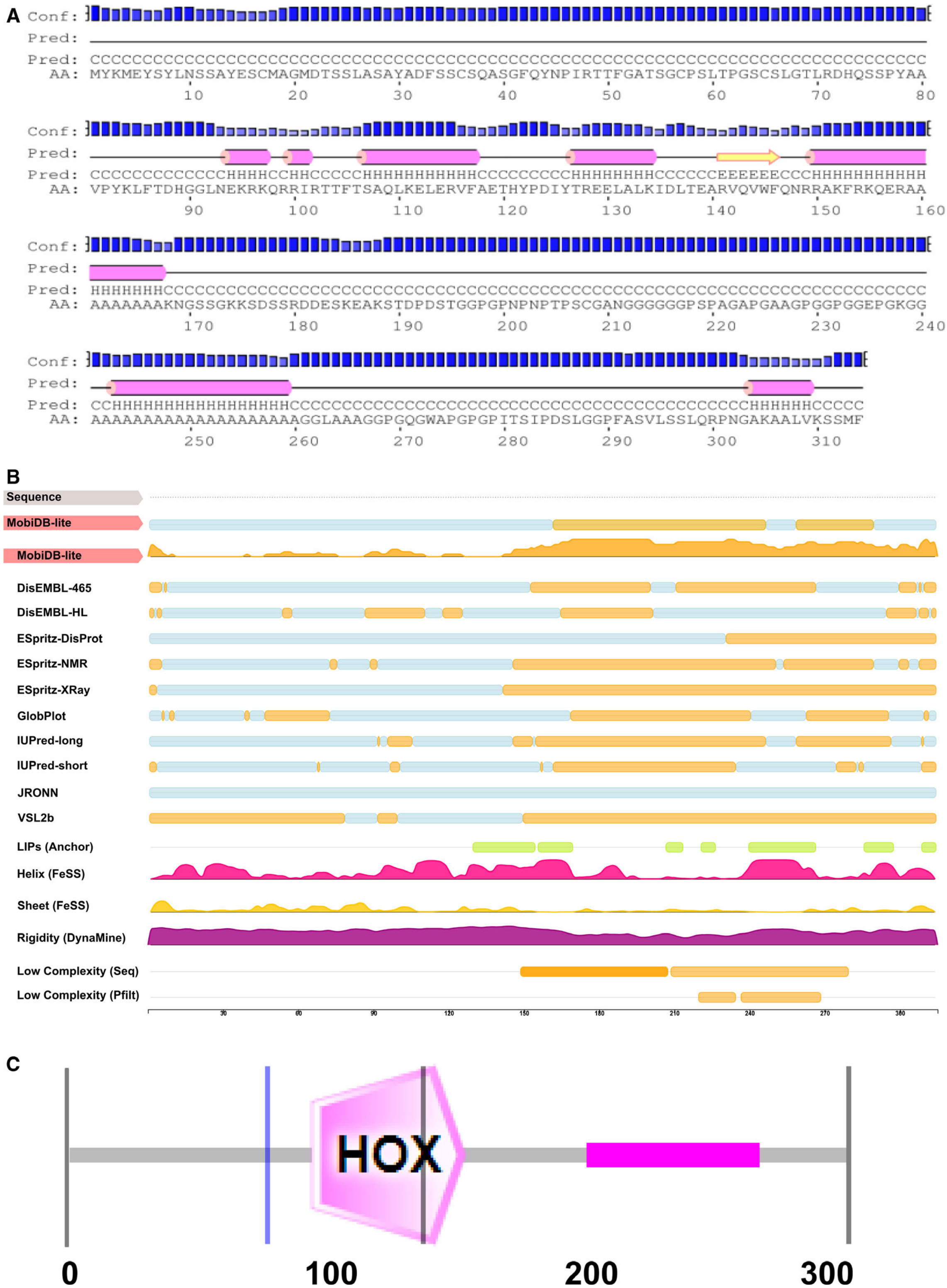

Fig. 2. (A) Primary structure of PHOX2B and prediction of secondary structure elements. Conf, confidence of prediction; C, coil; E, strand; H, helix. (B) Sequence analyzed by MOBIDB software: http://mobidb.bio.unipd.it/Q99453/predictions: unstructured regions (orange); structured regions (light blue). (C) Sequence elaborated by SMART program: HOX=HD domain: region 98–160; low complexity region: sequence 209–279 (purple).

The SDS/PAGE analysis of purified PHOX2B variants differing in the polyAla stretch (which theoretical mass is in the 20.9–22.8 kDa range) showed a single band of ~ 30 kDa (Fig. 3). This aberrant migration is a hallmark of intrinsically disordered proteins and is often due to their high content of acidic and negatively charged residues [25]. In the case of PHOX2B, the higher apparent molecular mass might originate from the largely unstructured C-terminal domain.

Insight into structural features of PHOX2B(20A) and its variants

The protein conformation of PHOX2B(20A), of the portions corresponding to its two main domains, and of the two variants related to the polyAla expansion was investigated by far-UV CD spectroscopy (Fig. 4). For all the proteins examined, the spectrum resembled the one typical of a α-helical-rich protein with two minima at 208 and 222 nm and a positive maximum at < 195 nm (Fig. 4A,B) in agreement with secondary structure predictions (Fig. 2). The spectrum corresponding to the C-terminal domain (Fig. 4A, dotted line) shows a decrease in the positive CD signal at around 195 nm, probably due to the consistent contribution of disordered regions. The similarity of the CD spectrum of PHOX2B(20A) with that of PHOX2B(0A) points to a similar secondary structure content while an alteration is apparent for the PHOX2B(27A) (Fig. 4B).

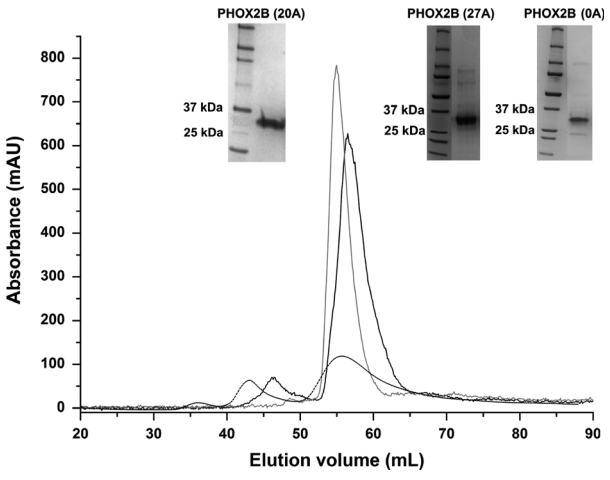

Fig. 3. Overlapping of elution profiles from a gel-permeation chromatography of 45 μM PHOX2B(20A) and its two variants; PHOX2B(20A) (black line), PHOX2B(0A) (light gray line) and PHOX2B(27A) (dashed line). In the inserts, the SDS/PAGE analysis of the three recombinant proteins present in the main peak is shown.

The stability of PHOX2B(20A) and its variants

The thermal stability of PHOX2B(20A) and its variants was also investigated by far-UV CD spectroscopy. The T_m values derived from temperature ramp denaturation curves following the CD signal at 220 nm are reported in Table 1. It is apparent that a strong stabilizing role of the HD region on the whole protein (18 °C decrease in T_m for the PHOX2B-Cter [HD deleted] variant), as well as a destabilization following the increase in the polyAla stretch in PHOX2B(27A).

The denaturation of PHOX2B variants differing in the polyAla stretch length was studied in the presence of chaotropic agents, such as guanidine hydrochloride (GdnHCl) and urea, to further investigate the role of this region on the whole protein. The PHOX2B variants 0A, 20A, and 27A displayed high resistance to both agents, as reported in Table 1.

The oligomeric state of PHOX2B(20A) and its variants

The size-exclusion chromatographic profile for the three PHOX2B variants differing in polyAla sequence points to an aggregation propensity for PHOX2B(27A) because of the presence of species eluting in the column void volume (~ 43–45 mL) and the low intensity of the peak corresponding to the monomeric protein (~ 55 mL), see Fig. 3. The difference in absorbance intensity between the elution profile of PHOX2B(27A) and the other two variants could be related to its strong tendency to aggregate and precipitate.

The oligomeric state of the PHOX2B variants was assessed using light scattering measurements. This analysis performed at 45 and 90 μM protein concentration demonstrated that all variants are monomeric in solution, with the only exception for PHOX2B(27A) which tends to oligomerize at increasing protein concentration (Fig. 5A–E and Table 2). The effect observed at higher protein concentration with the 27A variant was not apparent for other PHOX2B variants (data not shown).

Considering the role of PHOX2B as transcription factor, further analyses were carried out in the presence of its DNA target. Proteins and ATTA2 oligonucleotide (MW = 15 650 Da) were mixed in a 1 : 1 molar ratio and subjected to light scattering experiments (Fig. 6). A peak was observed for PHOX2B(20A) (Fig. 6A) and PHOX2B(0A) (data not shown) with a mass of ~ 50 kDa corresponding to a dimer in complex with its DNA target. On the contrary, the behavior of PHOX2B (27A) was different, forming a high molecular mass complex of ~ 200 kDa in the presence of DNA (Fig. 6B).

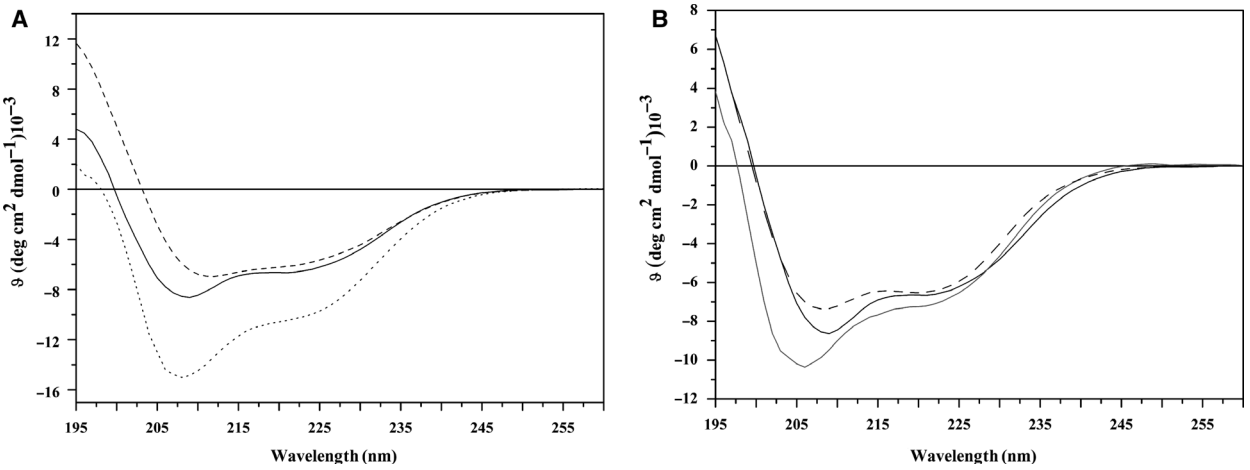

Fig. 4. Far-UV CD spectra (recorded at 10 °C) of: (A) PHOX2B(20A) (black line), HD domain (dashed line) and C-terminal domain (dotted line); (B) PHOX2B(20A) (black line), PHOX2B(0A) (light gray line), and PHOX2B(27A) (dashed line).

Table 1. Thermal and chemical denaturation of PHOX2B variants. n.d., not determined.

Protein	Melting temperature (°C)	c/2 (M)	
		Urea	GdnHCl
PHOX2B (20A)	48 ± 1	3.5 ± 0.1	3.0 ± 0.2
PHOX2B (0A)	47 ± 2	3.5 ± 0.1	3.5 ± 0.1
PHOX2B (27A)	40 ± 1	4.0 ± 0.2	3.2 ± 0.2
PHOX2B-HD	43 ± 2	n.d.	n.d.
PHOX2B-Cter	30 ± 2	n.d.	n.d.

Our results revealed that the polyAla expansion induces the formation of oligomers especially in the presence of DNA. On the contrary, DNA binding to the PHOX2B variant containing the correct number of alanine favors a conformational change leading to the formation of homodimers.

Conformational changes upon DNA binding

To get insight into PHOX2B(20A) structural changes in the presence of DNA, circular dichroism, chemical cross-linking, and limited proteolysis experiments were carried out. The specific binding of 10 μM PHOX2B (20A) to ATTA2 was studied by means of CD spectroscopy and the ratio of the ellipticity at 220 and 208 nm ([θ]220/208) was reported as a function of the amount of DNA added up to a stoichiometrically quantity of protein and DNA (Fig. 7A). The figure shows an increase in the ratio until it reached the characteristic value of ~ 1.0 after adding 5 μM DNA, as an effect of the reorganization of the helical structures. This result suggests the formation of a dimer involving a coiled-coil interaction [26,27].

Dissociation constant (K_d) for protein–DNA complex was determined by titrating PHOX2B(20A) with increasing amounts of ATTA2 oligonucleotide and by monitoring the binding following the quenching of intrinsic Trp fluorescence (Fig. 8). PHOX2B has two tryptophan residues at positions 145 (in the homeodomain) and 273 (in the C-terminal domain, downstream the 20-alanine stretch). In the absence of DNA, PHOX2B(20A) has an emission spectrum with a peak at ~ 349 nm. Upon binding of PHOX2B(20A) to DNA, a red-shift occurs in the emission spectra, shifting the maximum to ~ 353 nm (Fig. 8A). The change in the steady-state emission intensity at 350 nm as a function of DNA concentration is shown in Fig. 8B and a single K_d of 2.1 ± 0.3 nM was determined.

The propensity to oligomerize was apparent in chemical cross-linking experiments performed with the homobifunctional amino-reactive reagent BS3. When PHOX2B(20A) was incubated with BS3 and the reaction products were separated on a denaturing polyacrylamide gel, multiple protein forms at increasing mass were observed (especially at the top of the gel, Fig. 7B, lanes 2–4). Notably, when the same experiment was performed in the presence of DNA (Fig. 7B, lanes 5–7), two predominant bands with an apparent molecular mass of ≥ 25 kDa (monomer) and ~ 50 kDa (dimer) were produced. The intensity of the band at ~ 50 kDa increased in the presence of ATTA2 oligonucleotide and the oligomeric forms observed in the absence of DNA disappeared (Fig. 7B), suggesting a preferential formation of a homodimeric species in the presence of DNA.

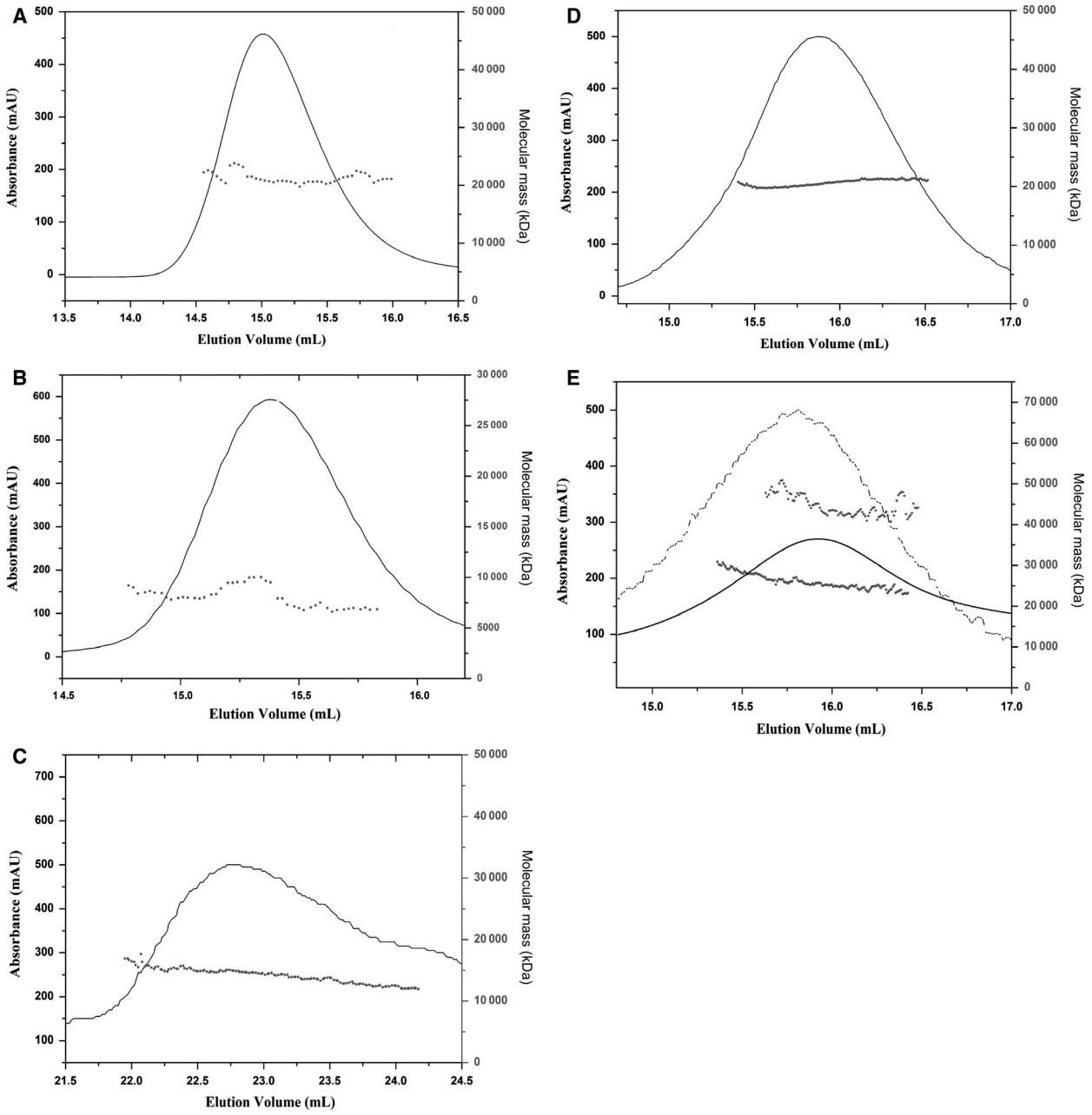

Fig. 5. Light scattering measurements of PHOX2B variants. The plots report the molecular mass (o) and absorbance at 280 nm (□) versus the elution volume for: (A) PHOX2B(20A); (B) HD domain; (C) C-terminal domain; (D) PHOX2B(0A); (E) PHOX2B(27A), at 45 μM (black line) and 90 μM (dashed line).

The interaction of PHOX2B(20A) with the ATTA2 oligonucleotide was then investigated by limited proteolysis incubating the protein in the presence of trypsin (at an enzyme:protein ratio of 1:1000). Comparing the time course of protein degradation in the absence (Fig. 6A, lanes 2–4) and in the presence of DNA (Fig. 9A, lanes 5–7), PHOX2B(20A) showed a different degradation pattern pointing to a conformational change altering the accessibility of the protein to trypsin digestion.

When the same experiment was carried out on PHOX2B(0A) and PHOX2B(27A) proteins different results were apparent (Fig. 9B,C). Concerning the effect of DNA binding, PHOX2B(0A) and PHOX2B (20A) were not affected by the presence of ATTA2 oligonucleotide. Indeed, under the conditions tested, a

Table 2. Light scattering (LS) analysis of PHOX2B (20A) and its variants.

Protein	Molecular mass		Ratio
	Theoretical[a] (Da)	Experimental (Da)	Exp/ Theor
PHOX2B (20A) 45 μM, 90 μM	22 297.60	22 590 ± 450	1
PHOX2B (0A) 45 μM, 90 μM	20 876.03	20 450 ± 110	1
PHOX2B (27A) 45 μM	22 795.16	21 460 ± 800	1
90 μM	22 795.16	42 600 ± 850	2
PHOX2B-HD 45 μM, 90 μM	8395.5	8813 ± 176	1
PHOX2B-Cter 45 μM, 90 μM	14 903.1	14 000 ± 100	1

[a] Calculated by PROTPARAM tool (http://web.expasy.org/protparam/).

lower amount of degradation products accumulated for the PHOX2B(0A) variant, suggesting a different fate for the digested fragments (Fig. 9B). On the other hand, the PHOX2B(27A) variant generated aggregates (visualized as bands at high molecular mass; Fig. 9C, compare lanes 2–7 vs lane 1) and was resistant to proteolytic digestion as indicated by the quantification of the 25 kDa band (Fig. 9C, bottom panel).

Degradation rates of PHOX2B(20A) and its variants

To examine the influence of polyAla expansion on the stability of PHOX2B at the cellular level, HeLa cells, which do not express endogenous PHOX2B, were transiently transfected with vectors expressing either PHOX2B(20A), PHOX2B(27A), or PHOX2B(0A) proteins tagged with HA. The protein turnover was analyzed by treating the cells with 1 $\mu g \cdot mL^{-1}$ of the

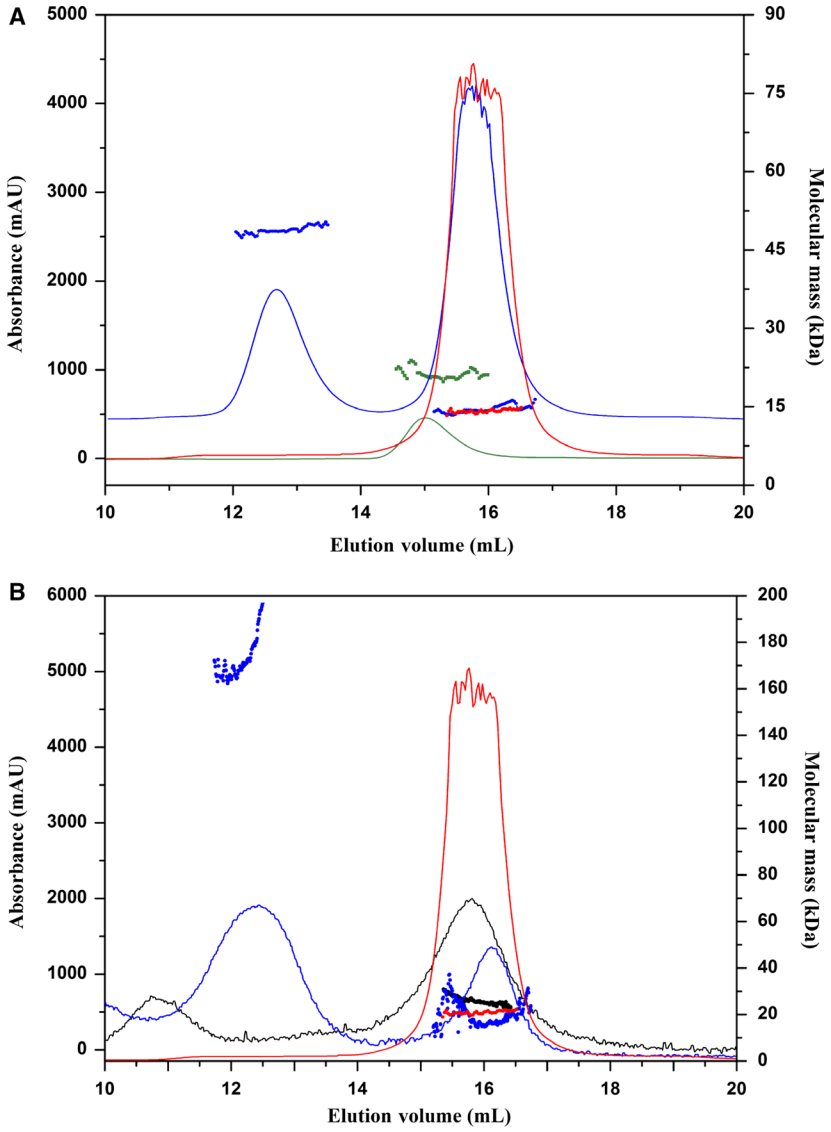

Fig. 6. Light scattering measurements of PHOX2B variants in the presence of DNA. The plots report the molecular mass (o) and absorbance at 280 nm (□) versus the elution volume for: (A) PHOX2B(20A) (green), the DNA (ATTA2 oligonucleotide, red) and the protein–DNA complex at a molar ratio 1 : 1 (blue); (B) PHOX2B(27A) (black), the DNA (ATTA2 oligonucleotide, red) and the protein-DNA complex at a 1 : 1 molar ratio (blue).

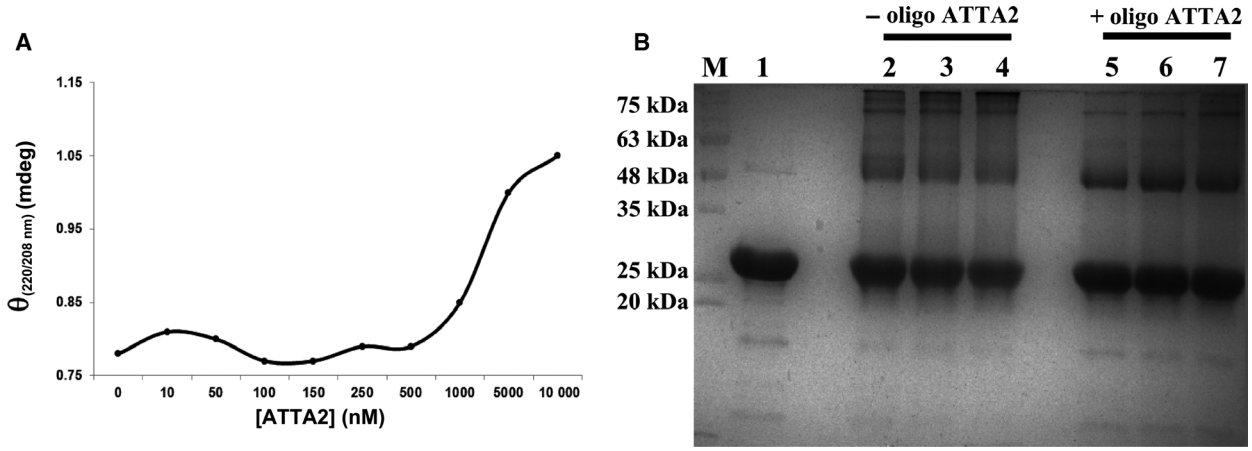

Fig. 7. Interaction studies between PHOX2B(20A) and DNA. A) The [θ]220 nm/208 nm ratio as function of increasing concentrations of ATTA2 oligonucleotide (0–10 μM). B) Chemical cross-linking of PHOX2B(20A) with 900 μM BS3 in the absence or presence of 22.5 μM ATTA2 oligonucleotide. A total of 45 μM PHOX2B(20A) was incubated with and without the cross-linker and analyzed on 15% SDS/PAGE. Lane M: molecular weight markers; lane 1: recombinant PHOX2B(20A); lanes 2–4 PHOX2B(20A) incubated for 0.5, 1, or 2 h in the presence of BS3 at a molar ratio of 1 : 20; lanes 5–7 PHOX2B(20A) incubated for 0.5, 1, or 2 h in the presence of both BS3 and DNA (protein : DNA molar ratio of 2 : 1).

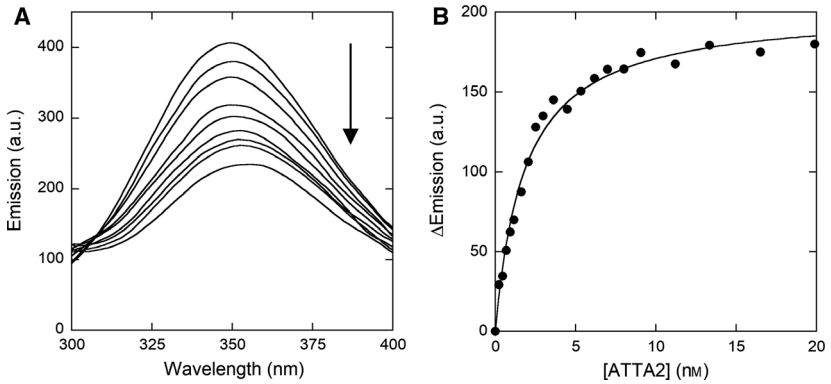

Fig. 8. Analysis of ATTA2 binding to PHOX2B(20A). (A) Effect of DNA binding to the fluorescence emission spectrum of 1 μM PHOX2B(20A) after adding increasing concentrations of ATTA2. (B) Change in the maximal intensity of protein fluorescence (~ 350 nm) at increasing DNA concentrations. Measurements were performed at 15 °C in 20 mM sodium phosphate, pH 7.4, 200 mM NaCl, 5% (v/v) glycerol, and 2 mM DTT.

inhibitor of protein synthesis cycloheximide (CHX). Western blot analysis of total lysates collected at different time points showed that PHOX2B(20A) has an half-life longer than 6 h (Fig. 10A,B) and the expansion of the polyAla tract increased the half-life of the protein (Fig. 10C,D). No difference in the degradation rate of PHOX2B(20A) and (0A) was observed (Fig. 10E,F), indicating that the deletion of the polyAla stretch does not modify the stability of the protein in the cell. The results indicate that the expansion of the polyAla tract significantly increases the cellular half-life of the protein.

Fibrils formation

Information about the potential formation of fibrils is gained through a fluorimetric assay that uses thioflavin T, exploiting its propensity to interpose in the regions rich in β sheets. PHOX2B(20A) and PHOX2B(27A) variants were incubated in the presence of thioflavin T at 37 °C and the change in fluorescence emission intensity at 485 nm was monitored over time. The variant PHOX2B(0A) showed a behavior comparable to that of PHOX2B(20A) (data not shown). In the case of the 27A-variant protein, after 4 days (96 h) the fluorescence intensity increases exponentially and reaches a stable value after 5 days (120 h) suggesting fibril formation (Fig. 11A). In the case of wild-type PHOX2B(20A), a less significant fluorescence increase is observed which is stable over time, putatively associated with the formation of protein aggregates.

In addition, the wild-type and variant PHOX2B samples diluted at 0.2 μM, were incubated at 37 °C at

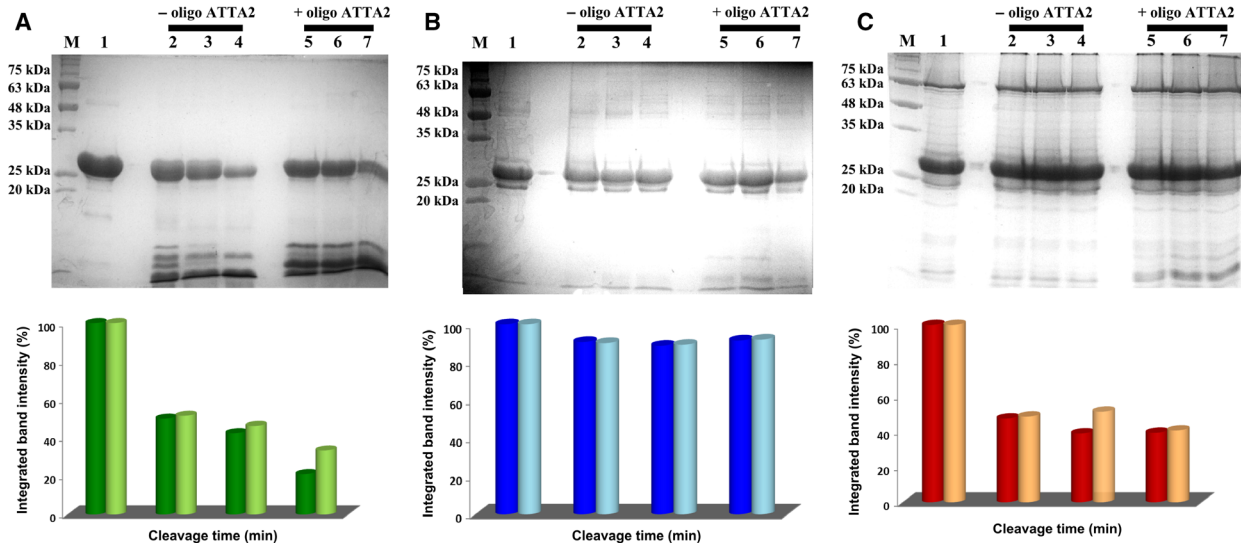

Fig. 9. Limited proteolysis analysis of: (A) PHOX2B(20A); (B) PHOX2B(0A); (C) PHOX2B(27A). Recombinant proteins were incubated with trypsin at room temperature at a protease: PHOX2B molar ratio of 1 : 1000, and at different times the reaction was stopped. Top: 18% SDS/PAGE. Lane M: molecular weight markers; lane 1: free recombinant protein (20 μg); lanes 2–4: proteins incubated for 10, 20, or 30 min with trypsin; lanes 5–7: proteins incubated for 10, 20, or 30 min with trypsin in the presence of DNA (protein : DNA molar ratio of 2 : 1). Bottom: intensity of the band at ~ 25 kDa (% vs time zero) plotted versus time of digestion.

a concentration of 10 μM in 20 mM sodium phosphate, 0.2 M NaCl, 2 mM dithiothreitol (DTT), pH 7.4, to acquire AFM images (Fig. 11 panels B–E). The morphology was observed at different stages of maturation and after 22 days (528 h). AFM images for PHOX2B (27A) show the presence of isolated fibrils (width ~ 20 nm, length ~ 1.5 μm) surrounded by amorphous aggregates of 20–40 nm in diameter (Fig. 11B). The analysis was repeated after 32 days (768 h) and the morphology was mainly characterized by the presence of mature fibrils which appear longer (> 2 μm) than those observed after 22 days and entangled, with a width ranging from 15 to 25 nm (Fig. 11C). On the other hand, the PHOX2B(20A) protein during the same observation period showed the presence of amorphous aggregates, with a diameter of 20–50 nm (Fig. 11 panels D, E).

Finally, our results indicate that the expansion of the polyAla tract in Phox2B induces the slow formation of fibrils *in vitro*.

Discussion

Congenital central hypoventilation syndrome is a rare neonatal disease, with a dominant autosomic genetic aetiology based on missense, nonsense, or frameshift mutations (10%) and polyAla triplet expansions (90%) of the paired-like homeobox gene *PHOX2B*. CCHS is defined by a failure of the autonomic control of breathing, associated with a broad variety of symptoms of autonomic nervous system dysfunction. The longer the stretch of alanine, the more severe is the respiratory phenotype. Therefore, this study focused on the biochemical characterization of the protein with the proper expansion in comparison with the mutated variant (PHOX2B(27A) involved in the insurgence of the pathology and with a variant lacking this polyAla region (PHOX2B(0A). The full-length, wild-type PHOX2B cannot be produced in a recombinant form as a folded protein able to bind DNA. Accordingly, and for the first time, five variants lacking the N-terminal part, predicted as an unstructured region, were expressed in *Escherichia coli* cells and purified to homogeneity. Three of them differed in the length of the second polyAla stretch and two were designed to express the homeodomain alone or the C-terminal region only (Fig. 1). *In vitro* studies on the purified proteins were used to clarify the mechanism by which pathogenic mutations affect the structure and correct folding of PHOX2B.

Among the PHOX2B variants generated in this work, the strongest decrease in stability was apparent for the C-terminal variant lacking both the N-terminal and the HD regions (Table 1): the HD domain seems to play a major role in protein stabilization and solubilization as also reported by [15]. Biochemical data highlight a higher sensitivity to thermal unfolding of the PHOX2B variant with the longest alanine stretch

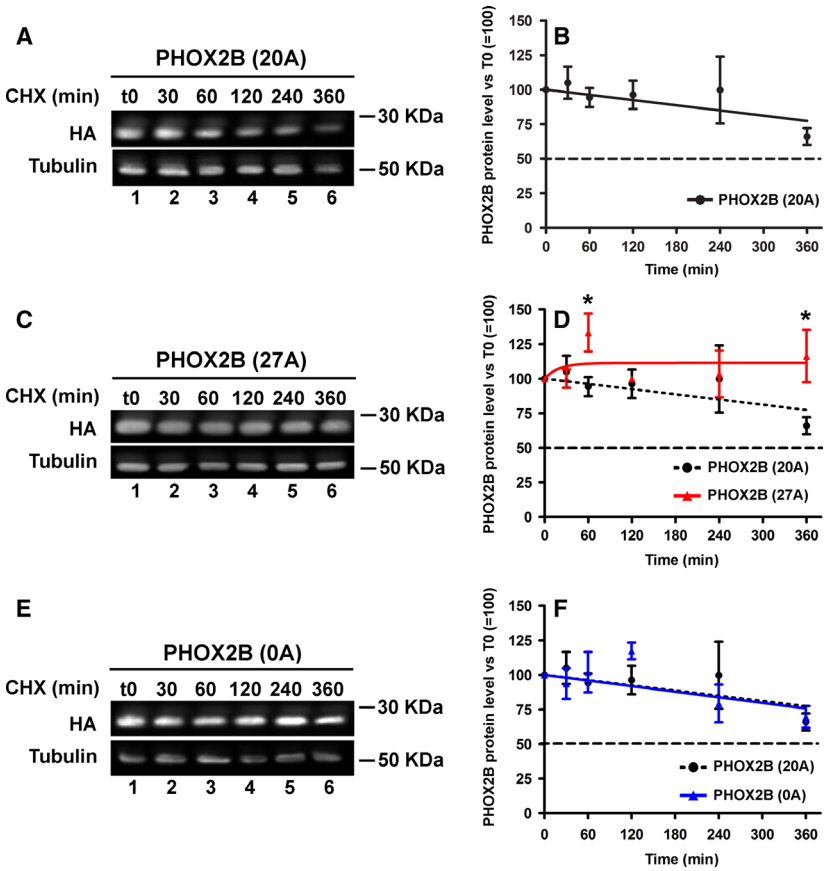

Fig. 10. Degradation rates of PHOX2B(20A) and its variants. (A, C, and E) representative western blots of total cell lysates from HeLa cells transfected with HA-tagged PHOX2B(20A) (panel A), PHOX2B(27A) (panel C), or PHOX2B(0A) (panel E) treated with 1 $\mu g \cdot mL^{-1}$ CHX for the indicated times (lanes 2–6). Lane 1: untreated cells. PHOX2B levels were determined by immunoblotting with anti-HA antibody. The PHOX2B signal was normalized to that of β-tubulin. (B, D, and F) Quantification: the graphs show the relative quantification of PHOX2B protein levels at each time point in comparison with time zero (= 100), that is, before adding CHX, and expressed as the mean densitometry intensity values ± SD (error bars) of each lane normalized to that of β-tubulin in two independent experiments. Nonlinear regression analysis was used to fit the experimental data to a one-phase exponential decay (GRAPHPAD PRISM 5.0). Statistically significant differences ($P < 0.05$, Student's *t*-test) in protein levels between PHOX2B(20A) and PHOX2B(27A) are indicated by *.

(27A) compared to wild-type (20A), that is, a 8 °C lower melting temperature, linked to a tendency to aggregate and precipitate. This is in agreement with literature data indicating that long polyAla stretches (> 23A) and homopolymeric tracts in general can easily form aggregates [28].

Among the recombinant proteins investigated here, the CD spectra show a slight alteration in secondary structure content for the PHOX2B(27A). Indeed, it is also the only variant prone to dimerization, a process dependent on the protein concentration. The increase in polyAla stretch strongly affects the interaction with DNA and our data clarify this feature from a structural point of view with the formation of non-functional aggregates. Gel permeation and LS measurements displayed that PHOX2B(20A) in complex with its DNA target forms a homodimer while the PHOX2B(27A) generated a high molecular mass complex. The propensity to aggregation of PHOX2B(27A) was evident also by chemical cross-linking and limited proteolysis experiments: because of the higher propensity to aggregate, the latter PHOX2B variant is more resistant to trypsin degradation. These results not only partially confirm previous investigations but also highlight significant differences, for example, previous studies reported that the length of the polyAla stretch affects the DNA binding only for expansions longer than 13 residues [14,15], and that the PHOX2B FL showed the propensity to generate oligomers (in details trimeric forms) [14]. These discrepancies probably arise from the different PHOX2B variants generated and the experimental conditions used. The self-interaction of expanded polyAla tracts favors an abnormal folding and, altering the interaction network, affects the normal function of a protein.

The *in vitro*-investigated folding, stability, and interaction properties of PHOX2B variants correlate with the cellular behavior. Previous papers showed that PHOX2B polyAla expansion induces the formation of protein aggregates that sequester ubiquitin and molecular chaperones (such as heat shock proteins) [14,18]. The observed increased stability in HeLa cells of the PHOX2B(27A) protein points to an alteration of the conventional degradation process, that can lead to the accumulation of the variant proteins that, by toxic gain of function and/or dominant-negative mechanisms, cause a general transcriptional dysregulation of those genes responsible for the correct development of the neural structure driving breathing control [11,24]. We speculate that CCHS is the result of the abnormal

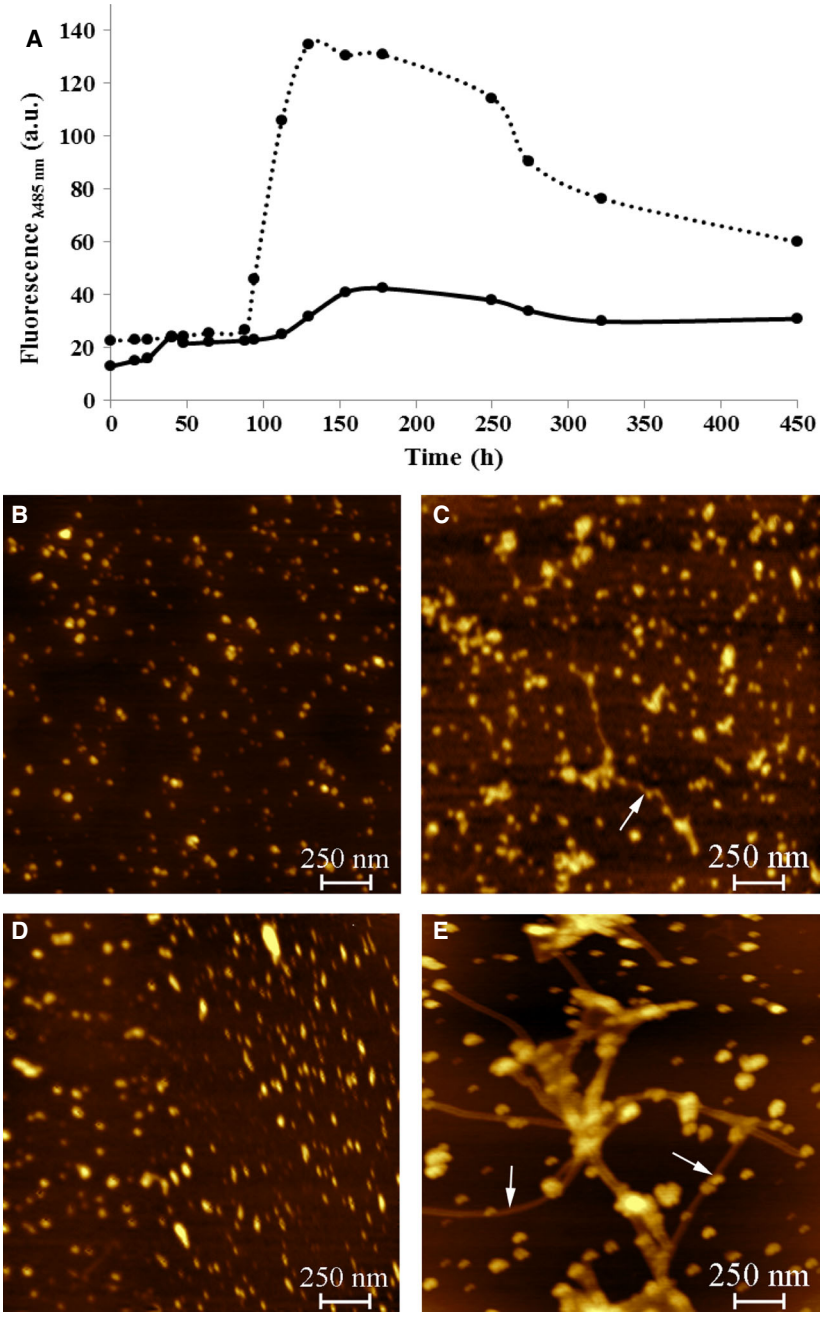

Fig. 11. (A) Aggregation behavior of 10 μM PHOX2B(27A) (dotted line) and PHOX2B (20A) (continuous line) at 37 °C assessed as thioflavin T fluorescence. AFM height images of PHOX2B(27A) (B, C) and PHOX2B(20A) (D, E) acquired after 22 days (528 h) (B, D) or 32 days (768 h) (C, E) of incubation at 37 °C. White arrows indicate location of fibril, at which the transverse width was measured. The scan size of each picture is 2 μm × 2 μm.

expression of PHOX2B target genes [24]. Moreover, increased accumulation of variant proteins, along with impairment of quality control system, can eventually lead to fibrils formation. Indeed, for the first time we demonstrated that the aggregates of PHOX2B(27A) are able to evolve in fibrils as demonstrated by fluorimetric assays in the presence of thioflavin T and AFM imaging.

Fibrils formation is not common to all proteins containing polyAla expansions [22], with the exception of PABPN1 that, conversely to the other polyAla containing proteins, cause a late-onset neurodegenerative disease. In this perspective, PHOX2B is the first polyAla containing protein associated with a congenital syndrome that shows fibrils formation, at least *in vitro*. As there is no evidence of visible aggregate formation in mice expressing PHOX2B +7Ala [19], the link between fibrils and the insurgence of CCHS needs to be further investigated. It is worth noting that the role of PHOX2B in adulthood has not been investigated, although in

mice Phox2b expression persists in most brainstem structures after birth [29]. Together with the findings that brain imaging and functional magnetic resonance imaging (fMRI) studies of CCHS patients suggest that other damages occur progressively, in addition to the developmental defects induced by PHOX2B mutations [30], we cannot exclude a role for fibrils in CCHS 'progression'. This evidence could pave the way for an innovative rational design of therapeutic drugs.

In conclusion, the longer polyAla stretch of the pathological PHOX2B variant could act as a nucleus for fibrils formation. If this process, in addition to decreasing the amount of soluble and active PHOX2B, triggers further events that concur to CCHS pathology is a point that merits further investigation.

Materials and methods

Cloning of PHOX2B wild-type and its variants

For the bacterial constructs, the synthetic cDNA encoding full-length human paired-like homeobox 2b (PHOX2B-FL) was designed by *in silico* back translation of the amino acid sequence reported in the database (NCBI Reference Sequence: NP_003915.2). Sequence corresponding to *NdeI* restriction site (CATATG), followed by six histidine codons and *Nhe*I restriction site (GCTAGC) was added to the 5′-end of cDNA; a *BamH*I (GGATCC) restriction site was inserted at the 3′-terminal. cDNA was synthesized by GeneArt (Life Technologies, Carlsbad, CA, USA), after codon optimization for the expression in *E. coli* (GeneBank accession number MK133750).

The gene was subcloned into the *Nde*I and *BamH*I restriction sites of the pET11a vector (Merck, Darmstadt, Germany), generating the pET11a-PHOX2B-FL plasmid. The recombinant PHOX2B-FL protein contains nine additional amino acids (MHHHHHHAS) at the N-terminal end, including the His_6-tag sequence, followed by alanine and serine residues coded by the recognition sequence of *Nhe*I restriction enzyme (Fig. 1A,B). The His-tag facilitated the purification procedure.

The PHOX2B variants were obtained by PCR using the primer design method reported by Liu and Naismith [31], Phusion High-Fidelity DNA Polymerase (Thermo Fisher Scientific™, Waltham, MA, USA), and buffer for GC-rich templates. All of the oligonucleotides used to generate the constructs are listed in Table S1. PHOX2B(20A) variant, in which the entire N-terminal domain of PHOX2B was deleted, was obtained inserting by PCR an additional *Nhe*I restriction site at the 5′-end of the homeodomain (HD) in the pET11a-PHOX2B-FL plasmid, digesting with *Nhe*I, and self-ligating the largest resulting DNA fragment. In a similar way, PHOX2B-Cter variant was generated inserting by PCR an additional *Nhe*I restriction site at the 5′-end of the C-terminal domain of PHOX2B in the pET11a-PHOX2B(20A) plasmid. The PHOX2B(27A) variant was obtained inserting a sequence coding for four additional residues of alanine to the pET11a- PHOX2B(20A) plasmid and using the resulting pET11a-PHOX2B(24A) plasmid as a template in a second mutagenesis reaction to insert a sequence coding for three additional residues of alanine (Table S1). The deletion of the polyAla stretch coding for 20 residues of alanine to produce PHOX2B(0A) variant was obtained using two-step of site-directed plasmid mutagenesis, producing, respectively, pET11a-PHOX2B(13A) and (0A), as reported in Table S1. The PHOX2B-HD variant was produced by replacing E157 with a stop codon (Table S1).

The generation of the mammalian expression plasmid HA-tagged PHOX2B(20A) has been described elsewhere [15]. The (27A) construct was obtained by digesting plasmid encoding the corresponding wild-type PHOX2B containing the normal alanine tract with the *PpuM*I restriction enzyme. The resulting 270-bp region, which encompasses the alanine tract, was replaced by the 291-bp region obtained using the same enzyme to digest the MYC-tagged PHOX2B +7Ala plasmid previously reported [11]. The HA-PHOX2B(0A) construct was generated using overlap extension PCR [32] with the HA-PHOX2B(20A) plasmid as the template. Briefly, two chimeric primers were used which consisted of an annealing fragment derived from one flanking region of the deletion and an anchor fragment derived from the flanking region on the other side of the deletion. The sequences of the primers for the upstream region are: forward external primer 5′-CAC AAG CTT GCT GCG GAA TTG TAC C-3′ and reverse 5′-AGG CCT CCG CCG CCC TTG CCG -3′; primers for the downstream region: forward 5′-AAG GGC GGC GGA GGC CTG GCT G -3′ and reverse external primer 5′-CTG ATA TCA TCG ATG AAT TCG GCT TCC-3′. The first PCR was performed using 40 ng of supercoiled plasmid containing PHOX2B(20A) cDNA to amplify two partially overlapping DNA fragments carrying the deletion. The two purified fragments were then annealed and used as the template (50 ng per each) for a second PCR step (using the external primers to obtain a single product). The PCR product was cloned after double enzymatic digestion with *Hind*III/*EcoR*V in the pcDNA3 vector (Invitrogen, Carlsbad, CA, USA). The PCR amplifications were performed using the GC-rich PCR system (Roche Applied Science, Penzberg, Germany), and all of the obtained DNA fragments were sequenced on both strands. All of the enzymes used for cloning were purchased from New England Biolabs (Ipswich, MA, USA).

Expression, and purification of PHOX2B and its variants

PHOX2B-FL

Full-length recombinant PHOX2B (PHOX2B-FL) was obtained using BL21(DE3)pLysS *E. coli* cells grown in TB medium at 37 °C, by inducing the protein expression with 1 mM isopropyl-β-D-thiogalactoside (IPTG) at $OD_{600\ nm} \sim 0.8$ and collecting the cells after 1 h of growth. The cell pellets were resuspended in 20 mM sodium phosphate, pH 7.4, 1 mM

pepstatin, 1 mM phenylmethylsulphonylfluoride (PMSF), 10 $\mu g \cdot mL^{-1}$ DNAse. PHOX2B-FL, containing a N-terminal His-tag, was purified by two chromatographic steps using denaturing conditions, because of the low recovery (2%) and purity obtained under native conditions. Crude extract was loaded on metal ion affinity chromatography (HiTrap TALON crude column equilibrated in 20 mM TrisHCl, pH 8.0, 0.3 M NaCl, 6 M GdnHCl, 10% (v/v) glycerol, 10 mM 2-mercaptoethanol, 1 mM pepstatin, 1 mM PMSF). Elution of bound protein was performed in 20 mM TrisHCl, pH 8.0, 0.3 M NaCl, 100 mM imidazole, 8 M urea, 10% (v/v) glycerol, 10 mM 2-mercaptoethanol, 1 mM pepstatin, 1 mM PMSF. Protein-containing fractions were loaded on size-exclusion chromatography (Superdex200 HiLoad 16/60 column equilibrated in 50 mM sodium phosphate, pH 6.8, 0.15 M NaCl, 4 M urea, 10% acetonitrile). The purification yield was 2 mg of protein per liter of culture. The purification of the PHOX2B-FL protein was achieved under denaturing conditions only. The protein was refolded by dilution in buffer with 0.1% (w/v) NLS: refolded PHOX2B did not bind DNA. Several attempts to remove NLS in order to recover a functional protein were unsuccessful. After dilution or dialysis to remove NLS the affinity of the protein for DNA is still too low for physiological activity (i.e., in the micromolar range) and the protein was unstable: protein precipitation was apparent during dialysis, ultrafiltration, or size-exclusion chromatography.

N-terminal deleted PHOX2B forms

Escherichia coli BL21(DE3) Gold strain (Invitrogen) was transformed with the recombinant vectors, grown at 37 °C, and protein expression was induced adding 0.5 mM IPTG (or 1 mM for PHOX2B(27A)) at an $OD_{600\ nm} \sim 0.8$ and growing for 3 h at 22 °C. The cell pellets were resuspended in 20 mM sodium phosphate, 1 M NaCl, 5% glycerol, 2 mM DTT, pH 7.4, containing a complete protease inhibitor cocktail (Roche). The extract was applied to a HisTrap HP column (GE Healthcare, Chicago, IL, USA) equilibrated with 20 mM sodium phosphate, 300 mM NaCl, 5% (vol/vol) glycerol, 2 mM DTT, 10 mM imidazole, pH 7.4. The column was washed with the same buffer plus 30 mM imidazole, and the bound proteins were eluted with the same buffer supplemented with 300 mM imidazole. Protein-containing fractions were pooled and loaded onto a Superdex 75 16/60 column (GE Healthcare) equilibrated in 20 mM sodium phosphate buffer (pH 7.4) containing 200 mM NaCl, 5% glycerol, 2 mM DTT.

The purification yield was approximately 5 mg per liter of culture for PHOX2B(20A) and PHOX2B(0A) and 2 $mg \cdot L^{-1}$ for PHOX2B(27A).

ATTA2 double-stranded oligonucleotide

DNA binding experiments were carried out using a double-stranded oligonucleotide corresponding to ATTA2 site of the PHOX2B promoter (25 bp, 5′-TAGTGTGATTGAAT TAAAGGGC AGG-3′) that has been shown to bind PHOX2B with high affinity [11,33].

Circular dichroism analyses

The CD spectra were recorded at 10 °C using a Jasco J-810 spectropolarimeter equipped with a Peltier thermostatic cell holder. Far-UV measurements (195–260 nm) were carried out using a 0.1-cm path length cell in 10 mM sodium phosphate, 100 mM NaCl, 2 mM DTT, pH 7.4, at a protein concentration of 10 μM [34]. Thermal denaturation was performed from 10 to 90 °C with an increment of temperature of 1 $°C \cdot min^{-1}$. Chemical denaturation was induced by GdnHCl or urea in the 0–6.0 M or 0–8.0 M range, respectively, incubating the samples for 1 h at room temperature. The unfolding process was monitored recording the CD signal at 220 nm. CD spectra were averaged over at least three independent scans and the baseline corrected by subtracting the buffer contribution [35].

For the titration with the DNA, far-UV spectra of 10 μM PHOX2B(20A) or its variants were recorded as stated above, in the presence of increasing concentrations (0–10 μM) of the double-stranded oligonucleotide (ATTA2). The baseline was corrected by subtracting the buffer and DNA contribution.

Light scattering (LS) analyses

For molecular mass measurements, static light scattering experiments were performed using a MiniDAWN Treos spectrometer (Wyatt Instrument Technology Corp., Santa Barbara, CA, USA) equipped with a laser operating at 658 nm and connected online to a size-exclusion chromatographic apparatus.

A 500-μL sample of purified 45 and 90 μM PHOX2B (20A) or its variants were loaded on a Superdex 75 10/30 column, equilibrated in 20 mM sodium phosphate, 200 mM NaCl, 5% glycerol, and 2 mM DTT, pH 7.4, and analyzed as described elsewhere [36]. A flow rate of 0.5 $mL \cdot min^{-1}$ was applied. Elution profiles were detected by a Shodex interferometric refractometer and data were analyzed by using ASTRA 5.3.4.14 software (Wyatt Technology, Santa Barbara, CA, USA).

For DNA interaction studies, 45 μM protein samples in 500 μL and 45 μM of double-stranded oligonucleotide (ATTA2) were loaded alone or in a 1 : 1 molar ratio in the same experimental conditions described above.

Spectrofluorimetry

Protein fluorescence measurements were performed in a Jasco FP-750 instrument. Protein emission spectra were taken from 300 to 400 nm (excitation at 280) and the fluorescence measurements were corrected for buffer contributions. Fluorescence measurements were performed at 0.03 $mg \cdot mL^{-1}$ protein concentration (corresponding to

$\sim$ 1 μM) in 20 mM sodium phosphate, pH 7.4, 200 mM NaCl, 5% (v/v) glycerol, 2 mM DTT, and at 15 °C. The protein–DNA dissociation constant (K_d) was estimated by titrating 1 μM protein with increasing amounts of DNA (from 200 pM to 20 nM DNA) and following the protein fluorescence quenching at 346 nm.

Cross-linking experiments

A total of 45 μM PHOX2B(20A) was incubated with or without 22.5 μM double-stranded oligonucleotides ATTA2 in the presence of 900 μM of bis(sulfosuccinimidyl) suberate (BS3) (1 : 20) in 20 mM sodium phosphate, 200 mM NaCl, 5% (vol/vol) glycerol, 2 mM DTT, pH 7.4, for 0.5, 1, or 2 h at room temperature (reaction volume of 20 μL). The samples were electrophoretically separated on a 18% (w/w) sodium dodecyl sulfate polyacrylamide gel (SDS/PAGE) [37].

Limited proteolysis studies

About 45 μM PHOX2B was incubated with or without 22.5 μM double-stranded oligonucleotide (ATTA2) with trypsin in a 1 : 1000 molar ratio. The proteolytic digestion was carried out for 10, 20, or 30 min at room temperature (reaction volume of 20 μL). The reaction was stopped by adding SDS loading buffer and boiling at 100 °C for 5 min, then the samples were separated on a 18% (w/w) SDS/PAGE.

The digital gel image of Coomassie-stained gel was acquired with ChemiDoc XRS System (Bio-Rad Laboratories, Milan, Italy) and the intensity of the bands was analyzed with the QUANTITYONE software (Bio-Rad Laboratories, Milan, Italy).

Cell cultures and transient transfections

The HeLa cells were grown in Dulbecco's modified Eagle's medium (Lonza, Basel, Switzerland) supplemented with 10% FBS (Euroclone, Milan, Italy), 100 units·mL^{-1} penicillin (Lonza), 100 μg·mL^{-1} streptomycin (Lonza), and 2 mM L-glutamine (Lonza) at 37 °C with 5% CO_2. The transfection experiments were performed by means of lipofection (FUGENE HD, Promega, Madison, WI, USA) using 1 × 10^5 HeLa cells (plated in 35 mm diameter wells) and 1 μg of each expression vector.

Assessment of the half-life of HA-tagged PHOX2B proteins

Forty-eight hours after transfection, protein stability was measured by means of treatment with 1 μg·mL^{-1} cycloheximide (CHX, Sigma-Aldrich, Saint Louis, MO, USA) for different times (0–360 min). The cells were collected by centrifugation, and lysed in concentrated 3X SDS-lysis buffer (6% SDS, 1% NP-40, 60 mM TrisHCl, pH 8.5, 10% (vol/vol) 2-mercaptoethanol, 25% (vol/vol) glycerol, 0.3% (w/vol) bromophenol blue) by incubation at 37 °C for 30 min with constant agitation. All samples were diluted to 1X SDS-lysis buffer and boiled 5 min at 100 °C. Viscosity was reduced by passing the sample through a syringe's (22 gauge) needle. Equal aliquots were then analyzed by western blot. The HA-tagged PHOX2B proteins were detected by means of primary rabbit anti-HA antibody (1:500; Sigma, catalog no. H6908), and β-tubulin by mouse anti-β-tubulin antibody (1:1000, Cell Signaling Technology, Danvers, MA, USA, D3U1W). Primary antibodies were revealed by infrared-conjugated rabbit IgG IRDye 800CW or mouse IgG IRDye 680CW (LI-COR Biosciences, Lincoln, NE, USA). Blots were scanned with the Odyssey CLx infrared imaging system (LI-COR Biosciences), and band intensities were determined with IMAGE STUDIO software (Li-Cor Biosciences). Data are expressed as the mean densitometry intensity values ± SD (error bars) of each lane normalized to that of β-tubulin, and shown as relative quantification of PHOX2B protein levels at each time point in comparison with time zero (= 100), that is, before adding CHX. Nonlinear regression analysis was used to fit the experimental data to a one-phase exponential decay. Data were analyzed by means of Student's *t*-test and the accepted level of significance was $P < 0.05$ (GRAPHPAD PRISM 5.0, San Diego, CA, USA).

Thioflavin T (ThT) assay fluorescence spectroscopy

The PHOX2B(20A) or PHOX2B(27A) were analyzed at a concentration of 10 μM in a solution containing 100 μM of thioflavin T in a final volume of 300 μL. The Varian Cary Eclipse spectrophotometer (Agilent, Santa Clara, CA, USA) and a 0.1-cm-diameter quartz cuvette were used to detect fibril formation. The samples were excited at a wavelength of 440 nm and the fluorescence emission spectrum was recorded between 450 and 600 nm. The samples were incubated at 37 °C and the fluorescence intensity change was monitored at 485 nm over time [38].

AFM studies

Both PHOX2B(20A) or PHOX2B(27A) were incubated at 37 °C at a concentration of 10 μM in 20 mM sodium phosphate, 0.2 M NaCl, 2 mM DTT, pH 7.4, and analyzed over time. The AFM images were obtained at room temperature in 'tapping' mode with a Bruker Multimode 8 microscope, using a tip with a radius of 8 nm, a resonance frequency of about 300 KHz, and an elastic constant of 50 N·m^{-1}. Samples for the AFM study were prepared by depositing 5 μL of an aqueous protein suspension (at 0.2 μM concentration to obtain a good visualization) on a mica substrate,

allowing the water to evaporate completely at room temperature.

Acknowledgements

This study was supported by the Telethon Foundation [grant No. GGP13055] to D.F., and the Associazione Italiana per la Sindrome da Ipoventilazione Centrale Congenita (A.I.S.I.C.C.). We are grateful to the Associazione Italiana per la Sindrome da Ipoventilazione Centrale Congenita (A.I.S.I.C.C.) and to all CCHS patients and their families. We also thank Ivan Ferrari and Luca De Luca for their helpful technical contribution.

Conflict of interest

The authors declare no conflict of interest.

Author contributions

LPi, LC, SdL, and RdG performed the experiments and analyzed the data; LPo, DF, SdG, RB, and EP conceived the project and wrote the paper.

References

1 Lavoie H, Debeane F, Trinh QD, Turcotte JF, Corbeil-Girard LP, Dicaire MJ, Saint-Denis A, Pagé M, Rouleau GA & Brais B (2003) Polymorphism, shared functions and convergent evolution of genes with sequences coding for polyalanine domains. *Hum Mol Genet* **12**, 2967–2979.

2 Amiel J, Trochet D, Clément-Ziza M, Munnich A & Lyonnet S (2004) Polyalanine expansions in human. *Hum Mol Genet* **13**(Spec No 2), R235–R243.

3 Albrecht A & Mundlos S (2005) The other trinucleotide repeat: polyalanine expansion disorders. *Curr Opin Genet Dev* **15**, 285–293.

4 Brown LY & Brown SA (2004) Alanine tracts: the expanding story of human illness and trinucleotide repeats. *Trends Genet* **20**, 51–58.

5 Messaed C & Rouleau GA (2009) Molecular mechanisms underlying polyalanine diseases. *Neurobiol Dis* **34**, 397–405.

6 Pattyn A, Morin X, Cremer H, Goridis C & Brunet JF (1999) The homeobox gene Phox2b is essential for the development of autonomic neural crest derivatives. *Nature* **399**, 366–370.

7 Pattyn A, Goridis C & Brunet JF (2000) Specification of the central noradrenergic phenotype by the homeobox gene Phox2b. *Mol Cell Neurosci* **15**, 235–243.

8 Stornetta RL, Moreira TS, Takakura AC, Kang BJ, Chang DA, West GH, Brunet JF, Mulkey DK, Bayliss DA & Guyenet PG (2006) Expression of Phox2b by brainstem neurons involved in chemosensory integration in the adult rat. *J Neurosci* **26**, 10305–10314.

9 Weese-Mayer DE, Berry-Kravis EM, Ceccherini I, Keens TG, Loghmanee DA, Trang H & Subcommittee ACCHS (2010) An official ATS clinical policy statement: congenital central hypoventilation syndrome: genetic basis, diagnosis, and management. *Am J Respir Crit Care Med* **181**, 626–644.

10 Di Lascio S, Benfante R, Di Zanni E, Cardani S, Adamo A, Fornasari D, Ceccherini I & Bachetti T (2018) Structural and functional differences in PHOX2B frameshift mutations underlie isolated or syndromic congenital central hypoventilation syndrome. *Hum Mutat* **39**, 219–236.

11 Di Lascio S, Bachetti T, Saba E, Ceccherini I, Benfante R & Fornasari D (2013) Transcriptional dysregulation and impairment of PHOX2B auto-regulatory mechanism induced by polyalanine expansion mutations associated with congenital central hypoventilation syndrome. *Neurobiol Dis* **50**, 187–200.

12 Bachetti T, Matera I, Borghini S, Di Duca M, Ravazzolo R & Ceccherini I (2005) Distinct pathogenetic mechanisms for PHOX2B associated polyalanine expansions and frameshift mutations in congenital central hypoventilation syndrome. *Hum Mol Genet* **14**, 1815–1824.

13 Bachetti T, Bocca P, Borghini S, Matera I, Prigione I, Ravazzolo R & Ceccherini I (2007) Geldanamycin promotes nuclear localisation and clearance of PHOX2B misfolded proteins containing polyalanine expansions. *Int J Biochem Cell Biol* **39**, 327–339.

14 Trochet D, Hong SJ, Lim JK, Brunet JF, Munnich A, Kim KS, Lyonnet S, Goridis C & Amiel J (2005) Molecular consequences of PHOX2B missense, frameshift and alanine expansion mutations leading to autonomic dysfunction. *Hum Mol Genet* **14**, 3697–3708.

15 Di Lascio S, Belperio D, Benfante R & Fornasari D (2016) Alanine expansions associated with congenital central hypoventilation syndrome impair PHOX2B homeodomain-mediated dimerization and nuclear import. *J Biol Chem* **291**, 13375–13393.

16 Wu HT, Su YN, Hung CC, Hsieh WS & Wu KJ (2009) Interaction between PHOX2B and CREBBP mediates synergistic activation: mechanistic implications of PHOX2B mutants. *Hum Mutat* **30**, 655–660.

17 Di Zanni E, Bachetti T, Parodi S, Bocca P, Prigione I, Di Lascio S, Fornasari D, Ravazzolo R & Ceccherini I (2012) In vitro drug treatments reduce the deleterious effects of aggregates containing polyAla expanded PHOX2B proteins. *Neurobiol Dis* **45**, 508–518.

18 Parodi S, Di Zanni E, Di Lascio S, Bocca P, Prigione I, Fornasari D, Pennuto M, Bachetti T & Ceccherini I (2012) The E3 ubiquitin ligase TRIM11 mediates the degradation of congenital central hypoventilation

syndrome-associated polyalanine-expanded PHOX2B. *J Mol Med (Berl)* **90**, 1025–1035.
19 Dubreuil V, Ramanantsoa N, Trochet D, Vaubourg V, Amiel J, Gallego J, Brunet JF & Goridis C (2008) A human mutation in Phox2b causes lack of CO2 chemosensitivity, fatal central apnea, and specific loss of parafacial neurons. *Proc Natl Acad Sci USA* **105**, 1067–1072.
20 Hughes JN & Thomas PQ (2013) Molecular pathology of polyalanine expansion disorders: new perspectives from mouse models. *Methods Mol Biol* **1017**, 135–151.
21 Shinchuk LM, Sharma D, Blondelle SE, Reixach N, Inouye H & Kirschner DA (2005) Poly-(L-alanine) expansions form core beta-sheets that nucleate amyloid assembly. *Proteins* **61**, 579–589.
22 Polling S, Ormsby AR, Wood RJ, Lee K, Shoubridge C, Hughes JN, Thomas PQ, Griffin MD, Hill AF, Bowden Q *et al.* (2015) Polyalanine expansions drive a shift into α-helical clusters without amyloid-fibril formation. *Nat Struct Mol Biol* **22**, 1008–1015.
23 Bernacki JP & Murphy RM (2011) Length-dependent aggregation of uninterrupted polyalanine peptides. *Biochemistry* **50**, 9200–9211.
24 Di Lascio S, Benfante R, Cardani S & Fornasari D (2018) Advances in the molecular biology and pathogenesis of congenital central hypoventilation syndrome-implications for new therapeutic targets. *Expert Opin Orphan Drugs* **6**, 719–731.
25 Hamdi K, Salladini E, O'Brien DP, Brier S, Chenal A, Yacoubi I & Longhi S (2017) Structural disorder and induced folding within two cereal, ABA stress and ripening (ASR) proteins. *Sci Rep* **7**, 15544.
26 Flemington E & Speck SH (1990) Evidence for coiled-coil dimer formation by an Epstein-Barr virus transactivator that lacks a heptad repeat of leucine residues. *Proc Natl Acad Sci USA* **87**, 9459–9463.
27 Kwok SC & Hodges RS (2004) Stabilizing and destabilizing clusters in the hydrophobic core of long two-stranded alpha-helical coiled-coils. *J Biol Chem* **279**, 21576–21588.
28 Oma Y, Kino Y, Toriumi K, Sasagawa N & Ishiura S (2007) Interactions between homopolymeric amino acids (HPAAs). *Protein Sci* **16**, 2195–2204.
29 Dauger S, Pattyn A, Lofaso F, Gaultier C, Goridis C, Gallego J & Brunet JF (2003) Phox2b controls the development of peripheral chemoreceptors and afferent visceral pathways. *Development* **130**, 6635–6642.
30 Harper RM, Kumar R, Macey PM, Harper RK & Ogren JA (2015) Impaired neural structure and function contributing to autonomic symptoms in congenital central hypoventilation syndrome. *Front Neurosci* **9**, 415. https://doi.org/10.3389/Fnins.2015.00415.
31 Liu H & Naismith JH (2008) An efficient one-step site-directed deletion, insertion, single and multiple-site plasmid mutagenesis protocol. *BMC Biotechnol* **8**, 91.
32 Ge L & Rudolph P (1997) Simultaneous introduction of multiple mutations using overlap extension PCR. *Biotechniques* **22**, 28–30.
33 Cargnin F, Flora A, Di Lascio S, Battaglioli E, Longhi R, Clementi F & Fornasari D (2005) PHOX2B regulates its own expression by a transcriptional auto-regulatory mechanism. *J Biol Chem* **280**, 37439–37448.
34 Caldinelli L, Molla G, Bracci L, Lelli B, Pileri S, Cappelletti P, Sacchi S & Pollegioni L (2010) Effect of ligand binding on human D-amino acid oxidase: implications for the development of new drugs for schizophrenia treatment. *Protein Sci* **19**, 1500–1512.
35 Pirone L, Esposito C, Correale S, Graziano G, Di Gaetano S, Vitagliano L & Pedone E (2013) Thermal and chemical stability of two homologous POZ/BTB domains of KCTD proteins characterized by a different oligomeric organization. *Biomed Res Int* **2013**, 162674.
36 Baglivo I, Pirone L, Pedone EM, Pitzer JE, Muscariello L, Marino MM, Malgieri G, Freschi A, Chambery A, Roop Ii R-M *et al.* (2017) Ml proteins from *Mesorhizobium loti* and MucR from Brucella abortus: an AT-rich core DNA-target site and oligomerization ability. *Sci Rep* **7**, 15805.
37 Contursi P, Farina B, Pirone L, Fusco S, Russo L, Bartolucci S, Fattorusso R & Pedone E (2014) Structural and functional studies of Stf76 from the Sulfolobus islandicus plasmid-virus pSSVx: a novel peculiar member of the winged helix-turn-helix transcription factor family. *Nucleic Acids Res* **42**, 5993–6011.
38 Malgieri G, D'Abrosca G, Pirone L, Toto A, Palmieri M, Russo L, Sciacca MFM, Tate R, Sivo V, Baglivo I *et al.* (2018) Folding mechanisms steer the amyloid fibril formation propensity of highly homologous proteins. *Chem Sci* **9**, 3290–3298.

Supporting information

Additional supporting information may be found online in the Supporting Information section at the end of the article.

Table S1. Primers used for mutagenesis.